

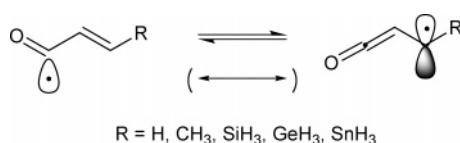
Theoretical Study on the Isomerization Behavior between α,β -Unsaturated Acyl Radicals and α -Ketenyl Radicals

Hiroshi Matsubara,^{*,†} Ilhyong Ryu,[†] and Carl H. Schiesser[‡]

Department of Chemistry, Faculty of Arts and Sciences, Osaka Prefecture University, Sakai, Osaka 599-8531, Japan, and School of Chemistry, Bio21 Molecular Science and Biotechnology Institute, The University of Melbourne, Victoria 3010, Australia

matsu@ms.cias.osakafu-u.ac.jp

Received December 2, 2004



Ab initio calculations using 6-311G**, cc-pVDZ, aug-cc-pVDZ, and a (valence) double- ζ pseudopotential (DZP) basis set, with (QCISD, CCSD(T)) and without (UHF) the inclusion of electron correlation, and density functional methods (BHandHLYP, B3LYP) predict that α,β -unsaturated acyl radicals and α -ketenyl radicals exist as isomers. At the CCSD(T)/cc-pVDZ//BHandHLYP/cc-pVDZ level of theory, energy barriers of 15.1 and 17.7–21.7 kJ mol⁻¹ are calculated for the isomerization of *s-trans*-propenoyl and *s-trans*-crotonoyl radical to ketenylmethyl and 1-ketenylethyl radical, respectively. Similar results are obtained for the reactions of *s-trans* isomers involving silyl, germyl, and stannyl groups with energy barriers (ΔE^\ddagger) of 12.2–12.4, 13.1–13.9, and 12.9–18.2 kJ mol⁻¹ at the CCSD(T)/DZP//BHandHLYP/DZP calculation, respectively. These results suggest that α,β -unsaturated acyl radicals and α -ketenyl radicals are not canonical forms but are isomeric species that can rapidly interconvert.

Introduction

Previous electron spin resonance (ESR) spectroscopic studies suggested that α,β -unsaturated acyl radicals exist as σ -type acyl radicals whose structures resemble the corresponding α,β -unsaturated aldehydes.^{1,2} For example, photolysis of bis[(*E*)-4,4-dimethylpent-2-enoyl]peroxide (**1**) at low temperature afforded both *s-trans* and *s-cis* rotamers of the (*E*)-4,4-dimethylpent-2-enoyl radical (Scheme 1). This study also revealed the *s-trans* structure to be the more stable conformation.³ On the other hand, recent rapid growth in the synthetic application of α,β -unsaturated acyl radicals produced by vinyl radical carbonylation^{4–6} has posed intriguing mechanistic questions surrounding the roles that α -ketenyl radical isomers play in the chemistry of the corresponding α,β -unsatur-

ated acyl radicals. For example, Pattenden and co-workers have shown (Scheme 2)⁷ that radicals formed by reaction of phenylseleno esters react exclusively via the α -ketenyl form and these radicals can be trapped efficiently by rapid intramolecular radical reactions such as 5-exo cyclization (eq 1)^{7a} and cyclopropylcarbiny radical ring opening (eq 2).^{7b}

Work in our laboratories has also shown that α -ketenyl radicals are generated during some radical cyclization processes (Scheme 3).⁶ For example, when *E*-3-iodo-allyl *tert*-butyl sulfide (**2**) was treated with carbon monoxide

(4) (a) Foster, R. E.; Larchar, A. W.; Lipscomb, R. D.; McKusick, B. C. *J. Am. Chem. Soc.* **1956**, *78*, 5606. (b) Nakatani, S.; Yoshida, J.; Isoe, S. *J. Chem. Soc., Chem. Commun.* **1992**, 880. (c) Okuro, K.; Alper, H. *J. Org. Chem.* **1996**, *61*, 5312. (d) Astley, M. P.; Pattenden, G. *Synlett* **1992**, 101. (e) Crich, D.; Chen, C.; Hwang, J.-T.; Yuan, H.; Papadatos, A.; Walter, R. I. *J. Am. Chem. Soc.* **1994**, *116*, 8937.

(5) (a) Ryu, I.; Hasegawa, M.; Kurihara, A.; Ogawa, A.; Tsunoi, S. *Synlett* **1993**, 143. (b) Ryu, I.; Okuda, T.; Nagahara, K.; Kambe, N.; Komatsu, M.; Sonoda, N. *J. Org. Chem.* **1997**, *62*, 7550. (c) Curran, D. P.; Sisko, J.; Balog, A.; Sonoda, N.; Nagahara, K.; Ryu, I. *J. Chem. Soc., Perkin Trans. 1* **1998**, 1591. (d) Ryu, I.; Miyazato, H.; Kuriyama, H.; Matsu, K.; Tojino, M.; Fukuyama, T.; Minakata, S.; Komatsu, M. *J. Am. Chem. Soc.* **2003**, *125*, 5632. (e) Tojino, M.; Ostuka, N.; Fukuyama, T.; Matsubara, H.; Schiesser, C. H.; Kuriyama, H.; Miyazato, H.; Minakata, S.; Komatsu, M.; Ryu, I. *Org. Biomol. Chem.* **2003**, *1*, 4262. (f) Tojino, M.; Uenoyama, Y.; Fukuyama, T.; Ryu, I. *Chem. Commun.* **2004**, 2482. (g) Uenoyama, Y.; Fukuyama, T.; Nobuta, O.; Matsubara, H.; Ryu, I. *Angew. Chem., Int. Ed.* **2005**, *44*, 1075.

* To whom correspondence should be addressed. Tel: +81-72-254-9720. Fax: +81-72-254-9931.

[†] Osaka Prefecture University.

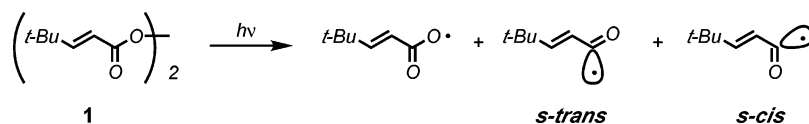
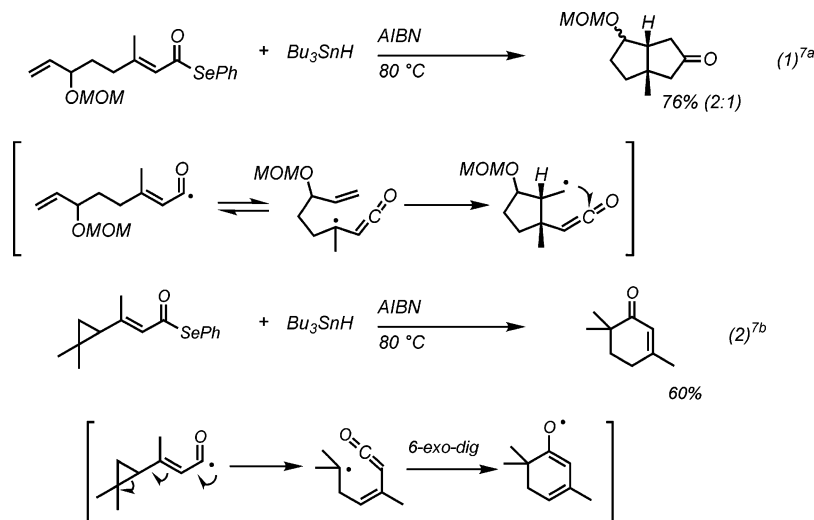
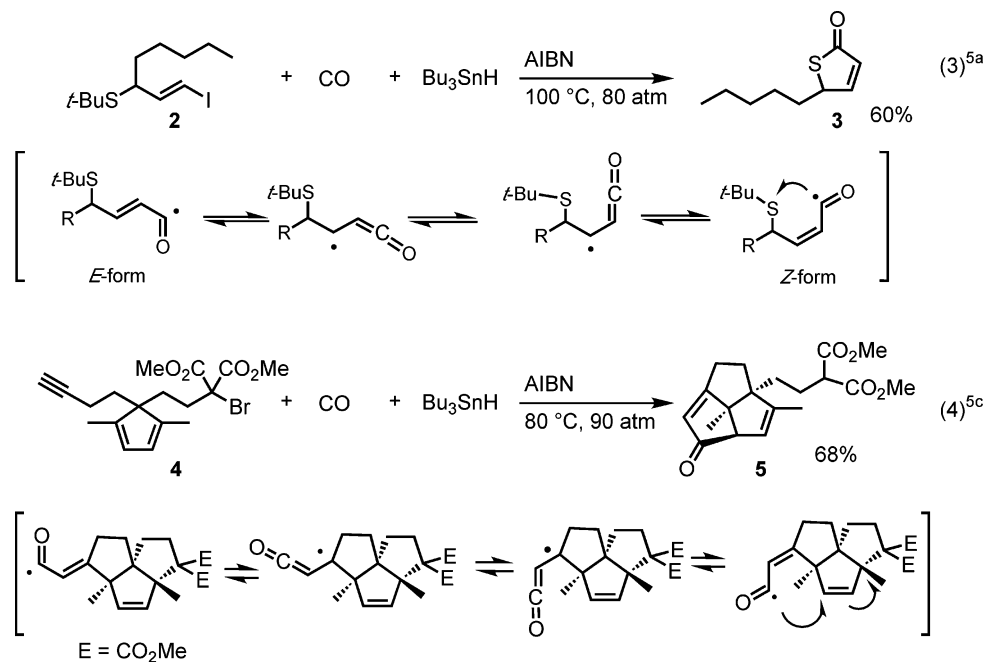
[‡] The University of Melbourne.

(1) (a) Davies, A. G.; Sutcliffe, R. *J. Chem. Soc., Perkin Trans. 2* **1980**, 819. (b) Davies, A. G.; Sutcliffe, R. *J. Chem. Soc., Chem. Commun.* **1979**, 473.

(2) A review on acyl radicals: Chatgililoglu, C.; Crich, D.; Komatsu, Ryu, I. *Chem. Rev.* **1999**, *99*, 1991.

(3) Korth, H.-G.; Luszyk, J.; Ingold, K. U. *J. Chem. Soc., Perkin Trans. 2* **1990**, 1997.

SCHEME 1

SCHEME 2. Isomerization Behaviors of α,β -Unsaturated Acyl Radicals in Tandem Radical Reactions via Noncarbonylation RouteSCHEME 3. Isomerization Behaviors of α,β -Unsaturated Acyl Radicals in Tandem Radical Reactions via Carbonylation Route

under radical conditions, α,β -unsaturated γ -thiolactone **3** was obtained as the sole product (eq 3).^{5a} Mechanistically, this outcome is only possible if the key reactive

intermediate is the *Z*-form of the appropriate unsaturated acyl radical.^{5b} Similarly, Ryu, Curran, and co-workers also encountered the *Z*-form of unsaturated acyl radicals in chemistry involving the bromide **4** to give exclusively the tricyclic product **5** (eq 4).^{5c} The isomerization of α,β -unsaturated acyl radicals via α -ketenyl radicals satisfactorily accounts for this result.

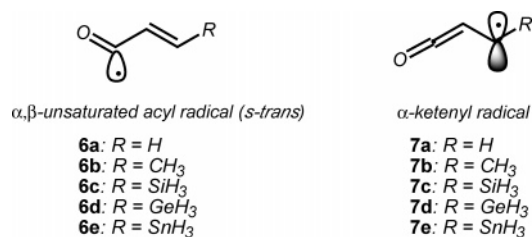
However, if one carefully considers mechanistic alternatives, each of the outcomes described above can also be explained in terms of a common delocalized intermedi-

(6) For reviews on radical carbonylations, see: (a) Ryu, I.; Sonoda, N. *Angew. Chem., Int. Ed. Engl.* **1996**, *35*, 1050. (b) Ryu, I.; Sonoda, N.; Curran, D. P. *Chem. Rev.* **1996**, *96*, 177. (c) Ryu, I. *Chem. Soc. Rev.* **2001**, *30*, 16.

(7) (a) Hayes, C. J.; Pattenden, G. *Tetrahedron Lett.* **1996**, *37*, 271. (b) Herbert, N.; Pattenden, G. *Synlett* **1997**, 69. (c) Harrington-Frost, N. M.; Pattenden, G. *Tetrahedron Lett.* **2000**, *41*, 403. (d) Harrington-Frost, N. M.; Pattenden, G. *Synlett* **1999**, 1917. (e) De Boeck, B.; Herbert, N.; Pattenden, G. *Tetrahedron Lett.* **1998**, *39*, 6971.

ate. Given this mechanistic uncertainty, and in order to shed further light on the chemistry of the species in question, we sought recourse to computational chemistry.

In this paper, we report that, consistent with similar studies by Guerra,⁸ computational methods generally predict that α -ketenyl radicals **7** are more stable than the corresponding α,β -unsaturated acyl radicals **6** using DFT methods such as B3LYP and BHandHLYP but less stable using correlated methods such as QCISD and CCSD(T). In addition, energy barriers between both types of radical species are calculated to be small suggesting that these species can interconvert readily.⁹ Importantly, these studies confirm that α -ketenyl and α,β -unsaturated acyl radicals are distinct species, rather than canonical forms of a common radical.



Methods

Ab initio and DFT calculations were carried out on Compaq Personal Workstation 600au, Alpha Station DS10L, DACS XJ-3000, and TX7/i9510 Itanium 2 computers using the Gaussian 98 and Gaussian 03 programs.¹⁰ Geometry optimizations were performed using standard gradient techniques at the SCF, BHandHLYP, and B3LYP levels of theory using unrestricted (UHF, UBHandHLYP, and UB3LYP) methods for open-shell

(8) Guerra, M. *Theor. Chem. Acc.* **2000**, *104*, 455.

(9) For calculations of some transition states for pentadienyl radical on semiempirical and Hartree-Fock levels, see: (a) Yamamoto, Y.; Ohno, M.; Eguchi, S. *J. Am. Chem. Soc.* **1995**, *117*, 9653. (b) Yamamoto, Y.; Ohno, M.; Eguchi, S. *J. Org. Chem.* **1996**, *61*, 9264. (c) Yamamoto, Y.; Noda, M.; Ohno, M.; Eguchi, S. *J. Org. Chem.* **1997**, *62*, 1292.

(10) (a) Frisch, M. J.; Trucks, G. W.; Schlegel, H. B.; Scuseria, G. E.; Robb, M. A.; Cheeseman, J. R.; Zakrzewski, V. G.; Montgomery, J. A., Jr.; Stratmann, R. E.; Burant, J. C.; Dapprich, S.; Millam, J. M.; Daniels, A. D.; Kudin, K. N.; Strain, M. C.; Farkas, O.; Tomasi, J.; Barone, V.; Cossi, M.; Cammi, R.; Mennucci, B.; Pomelli, C.; Adamo, C.; Clifford, S.; Ochterski, J.; Petersson, G. A.; Ayala, P. Y.; Cui, Q.; Morokuma, K.; Malick, D. K.; Rabuck, A. D.; Raghavachari, K.; Foresman, J. B.; Cioslowski, J.; Ortiz, J. V.; Stefanov, B. B.; Liu, G.; Liashenko, A.; Piskorz, P.; Komaromi, I.; Gomperts, R.; Martin, R. L.; Fox, D. J.; Keith, T.; Al-Laham, M. A.; Peng, C. Y.; Nanayakkara, A.; Gonzalez, C.; Challacombe, M.; Gill, P. M. W.; Johnson, B. G.; Chen, W.; Wong, M. W.; Andres, J. L.; Head-Gordon, M.; Replogle, E. S.; Pople, J. A. *Gaussian 98*, revision A.7; Gaussian, Inc.: Pittsburgh, PA, 1998. (b) Frisch, M. J.; Trucks, G. W.; Schlegel, H. B.; Scuseria, G. E.; Robb, M. A.; Cheeseman, J. R.; Montgomery, J. A., Jr.; Vreven, T.; Kudin, K. N.; Burant, J. C.; Millam, J. M.; Iyengar, S. S.; Tomasi, J.; Barone, V.; Mennucci, B.; Cossi, M.; Scalmani, G.; Rega, N.; Petersson, G. A.; Nakatsuji, H.; Hada, M.; Ehara, M.; Toyota, K.; Fukuda, R.; Hasegawa, J.; Ishida, M.; Nakajima, T.; Honda, Y.; Kitao, O.; Nakai, H.; Klene, M.; Li, X.; Knox, J. E.; Hratchian, H. P.; Cross, J. B.; Adamo, C.; Jaramillo, J.; Gomperts, R.; Stratmann, R. E.; Yazyev, O.; Austin, A. J.; Cammi, R.; Pomelli, C.; Ochterski, J. W.; Ayala, P. Y.; Morokuma, K.; Voth, G. A.; Salvador, P.; Dannenberg, J. J.; Zakrzewski, V. G.; Dapprich, S.; Daniels, A. D.; Strain, M. C.; Farkas, O.; Malick, D. K.; Rabuck, A. D.; Raghavachari, K.; Foresman, J. B.; Ortiz, J. V.; Cui, Q.; Baboul, A. G.; Clifford, S.; Cioslowski, J.; Stefanov, B. B.; Liu, G.; Liashenko, A.; Piskorz, P.; Komaromi, I.; Martin, R. L.; Fox, D. J.; Keith, T.; Al-Laham, M. A.; Peng, C. Y.; Nanayakkara, A.; Challacombe, M.; Gill, P. M. W.; Johnson, B.; Chen, W.; Wong, M. W.; Gonzalez, C.; Pople, J. A. *Gaussian 03*, revision B.05; Gaussian, Inc.: Pittsburgh, PA, 2003.

systems.¹¹ All ground and transition states were verified by vibrational frequency analysis. Further single-point QCISD and CCSD(T) calculations were performed on each of the BHandHLYP-optimized structures. When correlated methods were used, calculations were carried out using the frozen core approximation. Values of $\langle s^2 \rangle$ never exceeded 0.86 before annihilation of quartet contamination (except for some UHF calculations) and all DFT calculations afforded $\langle s^2 \rangle$ of less than 0.79. Where appropriate, zero-point vibrational energy (ZPE) corrections have been applied. Standard basis sets were used, as well as the (valence) double- ζ pseudopotential basis sets of Hay and Wadt¹² supplemented with a single set of *d*-type polarization functions for the heteroatoms in this study (exponents $d(\zeta)_{\text{Si}} = 0.284$,¹³ $d(\zeta)_{\text{Ge}} = 0.220$,¹³ and $d(\zeta)_{\text{Sn}} = 0.200$), together with the double- ζ all-electron basis sets of Dunning¹⁴ with an additional set of polarization functions (exponents $d(\zeta)_{\text{C}} = 0.75$, $d(\zeta)_{\text{O}} = 0.85$ and $p(\zeta)_{\text{H}} = 1.00$) for C, O, and H. We refer to this basis set as DZP throughout this work.¹⁵ In previous work, results generated using DZP proved to be very similar to those obtained using 6-311G** for reactions involving chlorine and silicon.¹⁵

Optimized geometries and energies for all structures of transition and ground states in this study (Gaussian Archive entries) are available as Supporting Information.

Results and Discussion

Isomerization of Propenoyl Radical to Ketenylmethyl Radical. We began our mechanistic studies by focusing on the isomerization of propenoyl radicals (**6a** (*s-trans*) and **10a** (*s-cis*)) to ketenylmethyl radical (**7a**). At the UHF and the BHandHLYP levels of theory employed for optimization, structures **6a**, **7a**, and **10a** were found to correspond to local minima (ground states) while **8a** and **9a** were found to correspond to the transition states for the appropriate isomerization reactions. Vibrational frequency analysis provided computational evidence for these structures as being true transition/ground states. Interestingly, at the B3LYP density functional method, neither the *s-cis* isomer **10a** nor the corresponding isomerization transition state **9a** involved in the isomerization of the *s-cis* isomer could be found. We have previously documented examples in which B3LYP calculations involving radical reactions provide data inconsistent with other theoretical treatments.¹⁶ We strongly recommend the use of benchmarking studies

(11) Hehre, W. J.; Radom, L.; Schleyer, P. v. R.; Pople, P. A. *Ab Initio Molecular Orbital Theory* Wiley: New York, 1986.

(12) (a) Wadt, W. R.; Hay, P. J. *J. Chem. Phys.* **1985**, *82*, 284. (b) Hay, P. J.; Wadt, W. R. *J. Chem. Phys.* **1985**, *82*, 270. (c) Hay, P. J.; Wadt, W. R. *J. Chem. Phys.* **1985**, *82*, 299.

(13) Höllwarth, A.; Böhme, M.; Dapprich, S.; Ehlers, A. W.; Gobbi, A.; Jonas, V.; Köhler, K. F.; Stegmann, R.; Veldkamp, A.; Frenking, G. *Chem. Phys. Lett.* **1993**, *208*, 237.

(14) Dunning, T. H.; Hay, P. J. In *Modern Theoretical Chemistry*; Schaefer, H. F., III, Ed.; Plenum: New York, 1977; Vol. 3, Chapter 1, pp 1–28.

(15) (a) Schiesser, C. H.; Smart, B. A.; Tran, T.-A. *Tetrahedron* **1995**, *51*, 3327. (b) Schiesser, C. H.; Wild, L. M. *J. Org. Chem.* **1998**, *63*, 670. (c) Schiesser, C. H.; Styles, M. L.; Wild, L. M.; *J. Chem. Soc., Perkin Trans. 2* **1996**, 2257. (d) Horvat, S. M.; Schiesser, C. H. *J. Chem. Soc., Perkin Trans. 2* **2001**, 939. (e) Horvat, S. M.; Schiesser, C. H.; Wild, L. M. *Organometallics* **2000**, *19*, 1239. (f) Matsubara, H.; Horvat, S. M.; Schiesser, C. H. *Org. Biomol. Chem.* **2003**, *1*, 1190. (g) Matsubara, H.; Schiesser, C. H. *J. Org. Chem.* **2003**, *68*, 9299. (h) Matsubara, H.; Schiesser, C. H. *Org. Biomol. Chem.* **2003**, *1*, 4335.

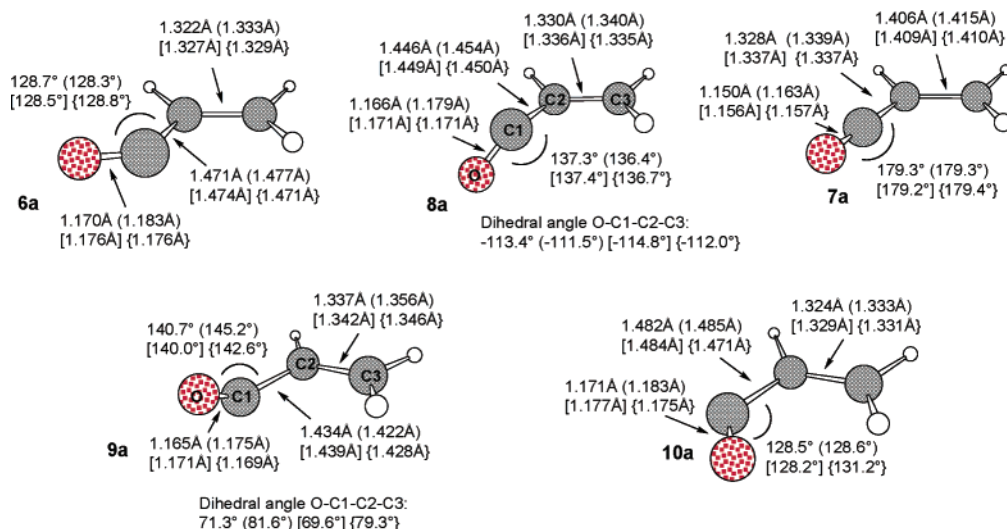


FIGURE 1. Optimized structure of acyl radicals **6a** and **10a**, ketenyl radical **7a**, and transition states **8a** and **9a**: BHandHLYP/6-311G**, (BHandHLYP/DZP), [BHandHLYP/cc-pVDZ], {BHandHLYP/aug-cc-pVDZ}.

SCHEME 4

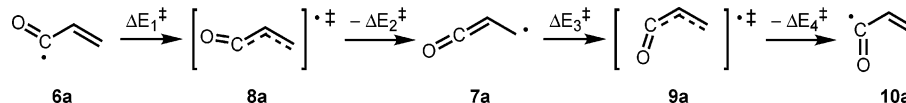


TABLE 1. Calculated Energy Barriers^a for the Forward (ΔE_1^\ddagger and ΔE_4^\ddagger) and Reverse (ΔE_2^\ddagger and ΔE_3^\ddagger) Isomerization of *s-trans* and *s-cis* Propenoyl Radical (**6a** and **10a**) to Ketenylmethyl Radical (**7a**) and Imaginary Frequencies^b of Transition States **8a** and **9a**

	ΔE_1^\ddagger	$\Delta E_1^\ddagger +$ ZPE	ΔE_2^\ddagger	$\Delta E_2^\ddagger +$ ZPE	ν	ΔE_3^\ddagger	$\Delta E_3^\ddagger +$ ZPE	ΔE_4^\ddagger	$\Delta E_4^\ddagger +$ ZPE	ν
UHF/6-31G*	12.3	7.4	9.5	10.7	239i	7.9	11.6	3.0	0.9	68i
UHF/6-311G**	12.4	7.5	14.3	15.1	252i	12.9	16.3	3.0	0.9	89i
UHF/DZP	12.2	7.4	7.5	8.8	226i	5.7	9.7	2.6	0.8	63i
BHandHLYP/6-311G**	13.9	9.3	18.5	18.9	260i	16.3	17.5	2.4	-0.5	120i
BHandHLYP/DZP	14.3	9.8	13.1	14.0	227i	11.0	11.1	3.7	-0.9	155i
BHandHLYP/cc-pVDZ	14.3	9.6	17.7	18.2	268i	15.5	17.0	3.0	-0.3	120i
BHandHLYP/aug-cc-pVDZ	13.1	8.8	12.9	13.8	230i	11.0	11.7	0.3	-3.2	73i
QCISD/cc-pVDZ//BHandHLYP/cc-pVDZ	15.2		7.4			5.7		6.1		
QCISD/aug-cc-pVDZ//BHandHLYP/aug-cc-pVDZ	14.2		2.8			2.8		4.6		
CCSD(T)/cc-pVDZ//BHandHLYP/cc-pVDZ	16.2		7.0			5.3		7.0		
CCSD(T)/aug-cc-pVDZ//BHandHLYP/aug-cc-pVDZ	15.1		2.6			2.6		5.6		
B3LYP/6-311G**	10.6	6.1	18.8	18.5	314i	c		c		
B3LYP/DZP	11.1	6.7	14.3	14.4	277i	c		c		
B3LYP/cc-pVDZ	10.9	6.4	17.9	17.6	319i	c		c		

^a Energies in kJ mol⁻¹. ^b Frequencies in cm⁻¹. ^c No transition states were found.

when applying B3LYP to radical systems; accordingly, this method was not used for the remaining radical reactions in this study.

The important geometric features of structures **6a**–**10a** calculated at BHandHLYP are shown in Figure 1 (results at other levels can be found in Figure S1 in the Supporting Information), while calculated energy barriers (ΔE_1^\ddagger , ΔE_2^\ddagger , ΔE_3^\ddagger , ΔE_4^\ddagger , Scheme 4) and corresponding imaginary frequencies are listed in Table 1. Full computational details are available in the Supporting Information.

Figure 1 reveals that acyl radicals **6a** and **10a** and ketenyl radical **7a** were predicted to be of C_s symmetry,

while transition states **8a** and **9a** were found to be of C_1 symmetry. Transition states **8a** and **9a** are predicted to involve carbonyl group bond angles in the range of 131–145°; these angles are slightly larger than those predicted for the acyl radicals **6a** and **10a**, while the geometry around the ketenyl carbon of **7a** is calculated to be almost linear, indicating that the transition states are closer in geometry to the acyl radical structures than to the corresponding ketenyl isomer. The carbonyl groups in the transition states are also calculated to deviate from the allylic plane; the dihedral angles of the oxygen atom to the allylic group are predicted to be in the range of 112–124° (**8a**) and 33–82° (**9a**). Inspection of Table 1 reveals that the calculated energy barriers (ΔE_1^\ddagger) for the “forward reaction” involving isomerization of the *s-trans* isomer to the ketenyl radical are calculated to be smaller than

(16) (a) Morihovitis, T.; Schiesser, C. H.; Skidmore, M. A. *J. Chem. Soc., Perkin Trans. 2* **1999**, 2041. (b) Falzon, C. T.; Ryu, I.; Schiesser, C. H. *Chem. Commun.* **2002**, 2338.

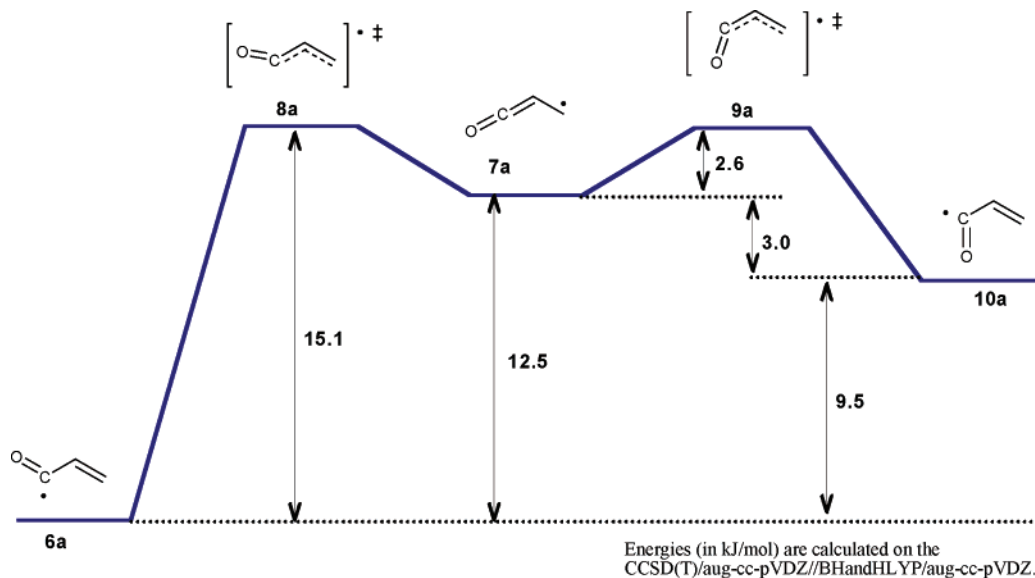


FIGURE 2. Reaction profile of isomerization of propenoyl radical.

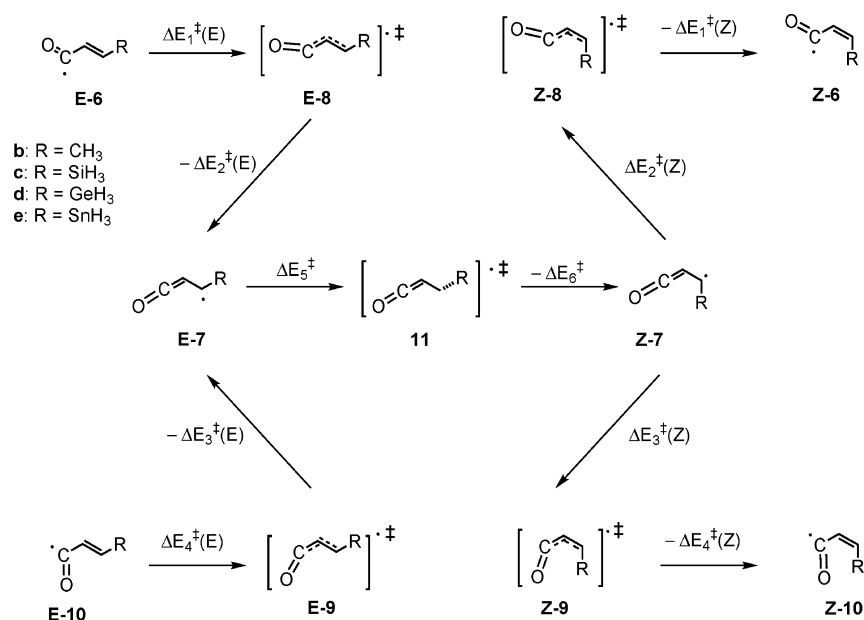
those for the reverse reaction (ΔE_2^\ddagger) at the UHF/6-311G**, BHandHLYP/6-311G**, BHandHLYP/cc-pVDZ levels of theory, as well as all B3LYP calculations. The remaining calculations, including high-level single point calculations, provide larger values for ΔE_1^\ddagger than for ΔE_2^\ddagger . At the highest level of theory used (CCSD(T)/aug-cc-pVDZ//BHandHLYP/aug-cc-pVDZ), a ΔE_1^\ddagger of 15.1 kJ mol⁻¹ is predicted for the isomerization of *s-trans* propenoyl radical to ketenylmethyl radical. In contrast, the calculated energy barriers (ΔE_4^\ddagger) for the “forward reaction” involving isomerization of the *s-cis* isomers are calculated to be smaller than those for the reverse reaction (ΔE_3^\ddagger) at the UHF and BHandHLYP levels of theory, while the high-level (QCISD, CCSD(T)) single-point calculations provided a larger ΔE_4^\ddagger than ΔE_3^\ddagger . These observations are consistent with those of Guerra who noted that the B3LYP DFT method severely overestimated the stabilization energies of ketenyl radicals compared to their α,β -unsaturated acyl isomers and that correlated methods such as CCSD(T), with or without geometry optimization, provided data consistent with available ESR observations. These results were interpreted by Guerra as suggesting that the CCSD(T) and DFT potential energy surfaces were sufficiently similar to allow meaningful single-point calculations to be performed.

The reaction profile of this isomerization calculated at the highest and most reliable level of theory is summarized in Figure 2. Inspection of Figure 2 reveals that the calculated energy barriers for the isomerization processes involving the *s-trans* and *s-cis* radicals (ΔE_1^\ddagger and ΔE_4^\ddagger) are 15.1 and 5.6 kJ mol⁻¹, respectively, indicating that these isomerizations are predicted to occur readily at ambient temperatures. Both of the acyl radicals (**6a**, **10a**) are calculated to be more stable than the ketenyl isomers; by 12.5 kJ mol⁻¹ for *s-trans* and 3.0 kJ mol⁻¹ for *s-cis* radical, and the *s-trans* radical is predicted to be more stable by 9.5 kJ mol⁻¹ than the *s-cis* radical. Therefore, the reaction equilibrium for these isomerization reactions favor the formation of the *s-trans*-propenoyl radical (**6a**).

Isomerization of Crotonoyl Radical to 1-Ketenylethyl Radical. Crotonoyl radical **6b** has two geometric isomers (*E* and *Z*) at the carbon–carbon double bond as well as *s-trans* and *s-cis* isomers at the acyl group. Therefore, the crotonoyl radical has four isomers, while 1-ketenylethyl radical **7b** has two stereoisomers. As shown in Scheme 5, *s-trans-E*-crotonoyl radical **E-6b** can isomerize to afford *E*-1-ketenylethyl radical **E-7b**, while *s-cis-E*-crotonoyl radical **E-10b** transforms to give **E-7b** as well. On the other hand, both *s-trans-Z*-crotonoyl radical **Z-6b** and *s-cis-Z*-crotonoyl radical **Z-10b** can isomerize in the same manner to the *E*-isomers giving *Z*-1-ketenylethyl radical **Z-7b**. The ketenyl radicals can transform into each other via transition state **11b**. Extensive searching of the C₄H₅O potential energy surface at the various levels of theory used in this study provided the data listed in Table 2. The important geometrical features of all structures relevant to this isomerization can be found in Figure S2 in the Supporting Information.

Inspection of Table 2 reveals that the energy barriers ($\Delta E_1^\ddagger(E)$, Scheme 5) for the forward reaction of the isomerization of the *s-trans-E*-crotonoyl radical **E-6b** to the *E*-1-ketenylethyl radical **E-7b** are calculated to be larger than those for the reverse reaction ($\Delta E_2^\ddagger(E)$) at all levels of theory employed, indicating that this reaction is endothermic. At the CCSD(T)/cc-pVDZ//BHandHLYP/cc-pVDZ level of theory the energy barriers are predicted to be at 21.7 kJ mol⁻¹ ($\Delta E_1^\ddagger(E)$) and 2.2 kJ mol⁻¹ ($\Delta E_2^\ddagger(E)$). The calculated energy barriers for the isomerization of the *s-cis-E*-crotonoyl radical **E-10b** to the *E*-1-ketenylethyl radical **E-7b** show the same trend; at the same level of theory, the energy barriers are predicted to be 16.5 kJ mol⁻¹ ($\Delta E_4^\ddagger(E)$) and 4.2 kJ mol⁻¹ ($\Delta E_3^\ddagger(E)$). On the other hand, the energy barriers ($\Delta E_1^\ddagger(Z)$) for the isomerization of the *s-trans-Z*-crotonoyl radical **Z-6b** to the *Z*-1-ketenylethyl radical **Z-7b** are also calculated to be larger than those for the reverse reaction ($\Delta E_2^\ddagger(Z)$) at all levels of theory employed, indicating that this reaction is also endothermic. At the CCSD(T)/cc-pVDZ//BHandHLYP/cc-pVDZ level of theory, the energy barriers are predicted

SCHEME 5


TABLE 2. Calculated Energy Barriers^a (ΔE^\ddagger ; Scheme 5) for Isomerization of Crotonyl Radical and the Corresponding Imaginary Frequencies^b (ν)

	$\Delta E_1^\ddagger(E)$	$\Delta E_1^\ddagger(E) +$ ZPE	$\Delta E_2^\ddagger(E)$	$\Delta E_2^\ddagger(E) +$ ZPE	ν	$\Delta E_3^\ddagger(E)$	$\Delta E_3^\ddagger(E) +$ ZPE	$\Delta E_4^\ddagger(E)$	$\Delta E_4^\ddagger(E) +$ ZPE	ν
UHF/6-311G**	18.4	12.7	18.4	12.7	209i	11.2	15.7	14.3	7.5	175i
BHandHLYP/cc-pVDZ	21.6	16.9	11.9	12.7	204i	10.3	10.2	11.2	5.5	216i
BHandHLYP/aug-cc-pVDZ// BHandHLYP/cc-pVDZ	20.6		6.0			5.9		9.4		
QCISD/cc-pVDZ//BHandHLYP/ cc-pVDZ	20.5		2.5			4.5		15.4		
CCSD(T)/cc-pVDZ//BHandHLYP/ cc-pVDZ	21.7		2.2			4.2		16.5		
	$\Delta E_1^\ddagger(Z)$	$\Delta E_1^\ddagger(Z) +$ ZPE	$\Delta E_2^\ddagger(Z)$	$\Delta E_2^\ddagger(Z) +$ ZPE	ν	$\Delta E_3^\ddagger(Z)$	$\Delta E_3^\ddagger(Z) +$ ZPE	$\Delta E_4^\ddagger(Z)$	$\Delta E_4^\ddagger(Z) +$ ZPE	ν
UHF/6-311G**	13.5	8.2	9.7	10.9	185i	7.8	11.3	2.5	-0.6	70i
BHandHLYP/cc-pVDZ	17.0	11.9	12.5	13.1	183i	10.7	10.9	6.8	1.7	190i
BHandHLYP/aug-cc-pVDZ// BHandHLYP/cc-pVDZ	15.5		7.5			7.0		3.7		
QCISD/cc-pVDZ//BHandHLYP/ cc-pVDZ	16.4		4.2			4.8		9.5		
CCSD(T)/cc-pVDZ//BHandHLYP/ cc-pVDZ	17.7		3.8			4.4		10.9		
		$\Delta E_5^\ddagger +$ ZPE		$\Delta E_5^\ddagger +$ ZPE		$\Delta E_6^\ddagger +$ ZPE		$\Delta E_6^\ddagger +$ ZPE		ν
UHF/6-311G**		31.8		35.7		33.4		32.3		132i
BHandHLYP/cc-pVDZ		43.6		40.5		45.0		41.5		230i
BHandHLYP/aug-cc-pVDZ// BHandHLYP/cc-pVDZ		43.0				44.5				
QCISD/cc-pVDZ//BHandHLYP/ cc-pVDZ		39.3				41.2				
CCSD(T)/cc-pVDZ//BHandHLYP/ cc-pVDZ		39.6				41.7				

^a Energies in kJ/mol. ^b Frequencies in cm⁻¹.

to be 17.7 kJ mol⁻¹ ($\Delta E_1^\ddagger(Z)$) and 3.8 kJ mol⁻¹ ($\Delta E_2^\ddagger(Z)$). Interestingly, and as previously commented on, the energy barrier ($\Delta E_4^\ddagger(Z)$) for the isomerization of the *s-cis*-*Z*-crotonyl radical **Z-10b** to the *Z*-1-ketenylethyl radical **Z-7b** is predicted to be smaller than that for the reverse reaction ($\Delta E_3^\ddagger(Z)$) at all levels of theory except high-level single point calculations (QCISD/cc-pVDZ//BHandHLYP/cc-pVDZ and CCSD(T)/cc-pVDZ//BHandHLYP/cc-pVDZ).

Apart from these results, the ketenyl radicals are calculated to be less stable than the corresponding crotonyl radicals at all levels of theory in this study. In addition and not unexpectedly, the *E*-crotonyl radicals (**E-6b**, **E-10b**) are predicted to be more stable than the *Z*-crotonyl radicals (**Z-6b**, **Z-10b**), while the *E*-1-ketenylethyl radical (**E-7b**) is calculated to be slightly less stable than the *Z*-1-ketenylethyl radical (**Z-7b**).

SCHEME 6

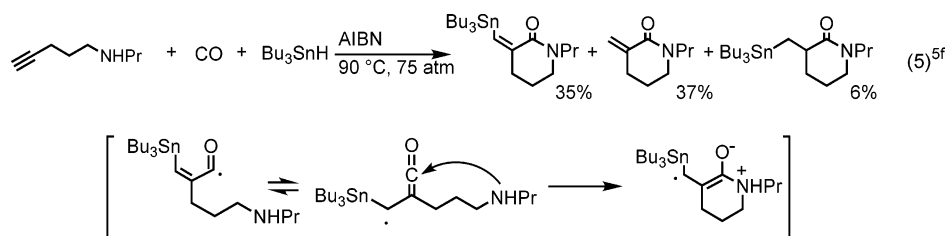


TABLE 3. CCSD(T)-Calculated Energy Barriers^a (ΔE^\ddagger ; Scheme 5) for the Isomerization of Silicon-, Germanium-, and Tin-Substituted Propenoyl Radicals

R	method	$\Delta E_1^\ddagger(E)$	$\Delta E_2^\ddagger(E)$	$\Delta E_3^\ddagger(E)$	$\Delta E_4^\ddagger(E)$	$\Delta E_1^\ddagger(Z)$	$\Delta E_2^\ddagger(Z)$	$\Delta E_3^\ddagger(Z)$	$\Delta E_4^\ddagger(Z)$	$\Delta E_5^\ddagger(Z)$	ΔE_6^\ddagger
SiH ₃	CCSD(T)/cc-pVDZ//BHandHLYP/cc-pVDZ	12.4	6.5	<i>b</i>	<i>b</i>	12.2	6.8	<i>b</i>	<i>b</i>	50.2	46.7
	CCSD(T)/DZP//BHandHLYP/DZP	10.7	16.3	<i>b</i>	<i>b</i>	12.2	16.8	<i>b</i>	<i>b</i>	52.8	49.8
GeH ₃	CCSD(T)/DZP//BHandHLYP/DZP	13.1	4.9	<i>b</i>	<i>b</i>	13.9	5.2	<i>b</i>	<i>b</i>	47.7	45.3
	CCSD(T)/DZP//BHandHLYP/DZP	12.9	4.7	0.1	2.7	18.2	4.1	3.7	15.9	44.8	48.6

^a Energies in kJ/mol. ^b No transition states were found.

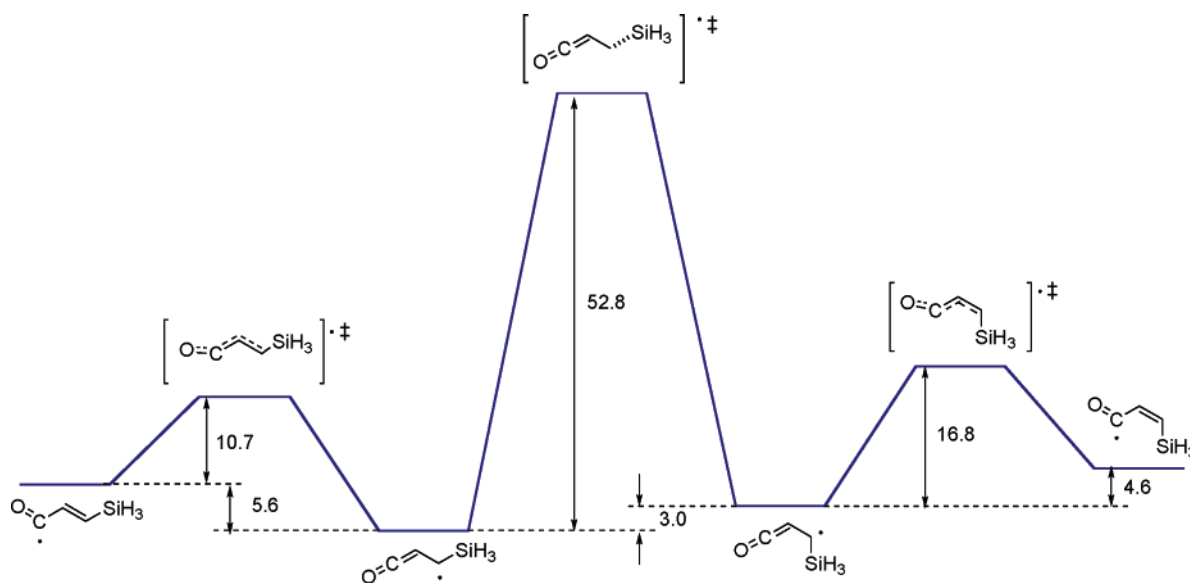


FIGURE 3. Reaction profile of isomerization of 3-silylpropenoyl radical. Energies (in kJ/mol) are calculated on the CCSD(T)/cc-pVDZ//BHandHLYP/cc-pVDZ.

Isomerization of 3-Silylpropenoyl, 3-Germylpropenoyl, and 3-Stannylpropenoyl Radical to Ketenylsilylmethyl, Ketenylgermylmethyl, and Ketenylstannylmethyl Radical. Recent work by some of us involved trapping of α -tributyltin substituted ketenyl radicals by amino groups^{5f,g} (Scheme 6). To provide further insight into this chemistry, specifically whether the key step of the reaction is likely to involve attack of the nitrogen at a ketenyl or acyl radical, we examined the isomerization of α,β -unsaturated acyl radicals bearing group XIV substituents by computational techniques.

Examination of the potential energy surfaces for the isomerization of the 3-silylpropenoyl **6c**, 3-germylpropenoyl **6d**, and 3-stannylpropenoyl **6e** radicals to the corresponding ketenyl species, namely the ketenylsilylmethyl **7c**, ketenylgermylmethyl **7d**, and ketenylstannylmethyl **7e** radicals were undertaken at the UHF/DZP and BHandHLYP/DZP levels of theory. In addition, for the silicon-containing species, the rearrangement reaction was also examined at the UHF/6-311G** and

BHandHLYP/cc-pVDZ levels of theory. The CCSD(T)-calculated energy barriers (Scheme 5) from this study are listed in Table 3 while a reaction profile for the isomerizations of **6c–7e** calculated at the CCSD(T)/cc-pVDZ//BHandHLYP/cc-pVDZ level is summarized in Figure 3. The important geometrical features of all structures relevant to the isomerization of acyl radicals involving silicon, germanium, and tin can be found in Figures S3, S4, and S5, respectively, in the Supporting Information, while calculated energy barriers at all levels of theory in this study and corresponding imaginary frequencies are listed in Table S1 in the Supporting Information.

It is of interest to note that at all of levels of theory employed, no *s-cis* isomers were found for radical **6c**, while both *E-s-cis* and *Z-s-cis* isomers were located in the case of the 3-stannylpropenoyl radical **6e**. In the case of the germanium-containing system, we were able to locate ground states of *s-cis* conformation for the 3-germylpropenoyl radical **6d** at all levels of theory employed in this study; while we were only able to locate a transition state

with *s-cis* conformation at the UHF/DZP level of theory for the isomerization of **6d**. Again, some high-level single-point calculations provided significantly lower energy barriers.

Interestingly, inspection of Table 3, Table S1 in the Supporting Information, and Figure 3 reveals that the substituted ketenyl radicals **7c–e** are predicted to be less stable than the isomeric propenoyl radicals at meaningful levels of theory, and the *Z*-ketenyl radicals are calculated to be slightly less stable than the *E*-ketenyl radicals. These results are to be compared with those obtained for the closely related crotonoyl system (see above). From this investigation, it is evident that inclusion of silyl, germyl and stannyl substituents has the effect of lowering the energy barriers for isomerization of the acyl species to the corresponding ketenyl radicals, while at the same time increasing the energy barriers for *E* to *Z* isomerization in the ketenyl radicals, when compared with the crotonoyl system. For example, at the CCSD-(T)/cc-pVDZ//BHandHLYP/cc-pVDZ level of theory, the energy barrier ($\Delta E_1^\ddagger(E)$) for the isomerization of *s-trans-E*-acyl radical **E-6b** to ketenyl radical **E-7b** is calculated to be 21.7 kJ mol⁻¹. Inclusion of the silyl substituent (**E-6c** → **E-7c**) lowers this barrier to 10.7 kJ mol⁻¹, while the barriers (ΔE_5^\ddagger) for the isomerization of ketenyl radicals **E-7b** and **E-7c** to **Z-7b** and **Z-7c** are calculated to be 39.6 and 52.8 kJ mol⁻¹, respectively.

Importantly, the computational data presented in this work indicate that α,β -unsaturated acyl radicals and

α -ketenyl radicals are not canonical forms but interconvertible isomers. Indeed, at all levels of theory employed in this study, energy barriers for the interconversion of these unsaturated radicals are calculated to be less than about 22 kJ mol⁻¹, indicating that α,β -unsaturated acyl radicals can easily transform into the corresponding α -ketenyl radicals and that in all likelihood, they will exist in equilibrium at the usual temperatures used in radical reactions.

Acknowledgment. We gratefully acknowledge the support of the Melbourne Advanced Research Computing Centre and Library & Science Information Center, Osaka Prefecture University. I.R. acknowledges a Grant-in-Aid for Scientific Research on Priority Areas (A) “Reaction Control of Dynamic Complexes” from the Ministry of Education, Culture, Sports, Science and Technology, Japan.

Supporting Information Available: Diagrams containing important geometrical features of all ground and transition states located at all levels of theory employed in this study (Figures S1–S5); calculated energy barriers for the isomerization of silicon-, germanium-, and tin-substituted propenoyl radical at all levels of theory employed in this study (Table S1); and Gaussian Archive entries for all optimized structures at all levels of theory employed in this study and higher-level single-point energies. This material is available free of charge via the Internet at <http://pubs.acs.org>.

JO047868I